
REPTRA: Mapping Immune T Cell Receptor Activity from Full Sequences with a Debiased Contrastive Loss

John Abel

Repertoire Immune Medicines
jabel@repertoire.com

Brinda Vijaykumar

Repertoire Immune Medicines
bvi jaykumar@repertoire.com

Neel Patel

Repertoire Immune Medicines
npatel@repertoire.com

Anthony J. Coyle

Repertoire Immune Medicines
tcoyle@repertoire.com

Christophe Benoist

Harvard Medical School
cb@hms.harvard.edu

Daniel C. Pregibon

Repertoire Immune Medicines
dpregibon@repertoire.com

Abstract

Contrastive learning is amenable to representing the vast space of interaction between highly specific T cell receptors (TCRs) and the epitopes to which they bind, potentially enabling diverse applications in immune engineering. However, progress in mapping TCR-epitope recognition has been limited by skewed datasets and training approaches that may exacerbate biases and obfuscate model performance. Furthermore, most TCR-epitope models represent only one of three complementarity-determining regions (CDRs) of the TCR, potentially limiting performance. Here, we present a CLIP-style contrastive-learning model for representation of epitopes and T cell receptor activity (REPTRA), incorporating a full TCR sequence representation and trained using a debiased InfoNCE loss. We demonstrate resulting improvements in performance, and perform ablations to identify the contributions of the modified loss and TCR representation. Furthermore, we apply an interpretability analysis to the REPTRA attention-pooling projection heads to reveal that CDR1 and CDR2, in addition to CDR3, are important for learning TCR-epitope recognition. In doing so, we develop a performant model for contrastive mapping of T cell receptor activity.

1 Introduction

The immune synapse is the biological interface central to the body’s cellular response in cancer, autoimmune disorders, and infectious disease. In the immune synapse, a T cell receptor (TCR) recognizes a peptide from a degraded protein presented on a cell’s surface by a major histocompatibility complex (MHC) molecule [1]. TCRs that recognize and bind specific peptide-MHCs (pMHCs) initiate an immune response. Deciphering the immune synapse would enable engineering a variety of immune therapies, e.g. beneficial activation of adaptive immunity (for TCR-mimic therapeutics) or modulation of immune response to self-antigens (for immune-tolerizing vaccines) [13, 16, 22]. However, this remains a challenge due to the diversity of synapse features. To date, approximately 10^{10} TCRs and 10^6 pMHCs have been described [24]. Machine learning approaches for deciphering the interaction of TCRs and pMHCs in the immune synapse from sequences, i.e. contrastive mapping, is therefore highly desirable.

Table 1: dataset composition for REPTRA training and evaluation, and comparison with the TULIP benchmark. Note that unique positive TCR-epitope pairs are reported, because negative sampling procedures may vary and duplicate positive pairs are included in the TULIP dataset. To demonstrate dataset skew, the number of TCRs pairing to the three most prevalent epitopes for the R-1 and TULIP datasets (respectively) are reported.

	Train	R-1 Val	Test	TULIP Test
Unique Positive Pairs (N)	13,634	2,352	2,754	854
TCRs (N)	12,254	2,101	2,451	853
Peptides (N)	4,416	767	793	148
KLGGALQAK (N, %)	1407 (10.3%)	305 (13.0%)	300 (10.9%)	0 (0.0%)
GILGFVFTL (N, %)	1036 (7.6%)	218 (9.3%)	420 (15.3%)	310 (36.3%)
RAFKKQLL (N, %)	316 (2.3%)	70 (3.0%)	80 (2.9%)	0 (0.0%)
NLVPMVATV (N, %)	121 (0.9%)	26 (1.1%)	47 (1.7%)	68 (8.0%)
GLCTLVAML (N, %)	271 (2.0%)	66 (2.8%)	75 (2.7%)	66 (7.7%)

Numerous recent studies have sought to directly predict TCR-epitope specificities with a variety of machine learning-based methods [4, 7, 8, 10, 11, 15, 17], and several have made significant progress in tackling this challenge. However, data composition and problem structure have posed significant challenges for applying machine learning in this space. Despite the wealth of available TCR sequences, reported TCR-pMHC interactions are limited. Few well-characterized epitopes (peptides presented by MHC) from common viral antigens such as influenza, Epstein-Barr virus, cytomegalovirus, and SARS-CoV-2 comprise the majority of large public databases of positive TCR-epitope interactions [21, 23]. Generating negative TCR-epitope interactions is additionally challenging: for example, sampling negative TCRs from a healthy TCR repertoire leads to distribution shift and loss of generalization (as identified in [15]). Contrastive learning suits the overall problem structure given the very low positive-to-negative interaction ratio, yet direct application of typical contrastive learning techniques where each positive TCR-epitope interaction is used to create a similarity matrix leads to a quadratic weighting of epitopes with respect to the number of occurrences of their corresponding TCRs. This results in a latent space biased toward the few highly studied antigens and potentially inflated performance metrics. If a model can accurately predict non-interactions for the few epitopes that comprise >50% of the test data, few-shot performance will appear strong, yet the model will fail in application.

In this study, we present several modifications to the TCR-epitope contrastive learning problem with a CLIP-style architecture. We contribute the following:

1. a contrastive model that leverages the entire TCR amino acid sequence with learned weighting via attention pooling,
2. epitope-frequency-debiased InfoNCE loss and evaluation metrics enabling improved contrastive learning of the TCR-epitope interaction space, and
3. empirical scaling and evaluation results on a larger TCR-epitope interaction dataset demonstrating the utility of these methods and identifying limitations.

Together, these methods enable training a performant model for contrastive representation of epitopes and T cell receptor activity (REPTRA).

2 Approach

2.1 Datasets

We aggregated multiple datasets for model training and evaluation. We selected all TCR-epitope pairs from the VDJdb database with a confidence score of 3 [21]. To reconstruct TCR alpha and beta subunit sequences from a given V-gene, J-gene, third complementarity-determining region (CDR3), and C-gene in VDJdb, we aligned the CDR3 amino acid sequences with the reference V/J/C-gene amino acid sequences from the Immunogenetics (IMGT) database [2] via CellRanger (10X

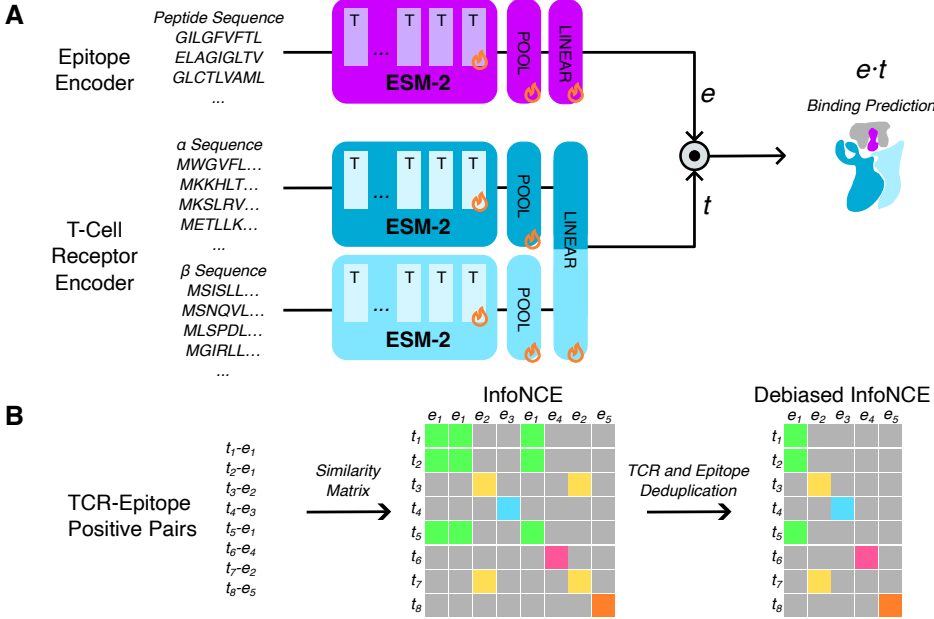


Figure 1: (A) schematic of REPTRA structure. Flames denote which blocks are trained. Note that the MHC is not explicitly encoded. (B) Visualization of debiased InfoNCE loss. By deduplicating epitopes and TCRs, we eliminate duplicate entries in the contrastive loss and evaluation.

Genomics). To significantly expand upon commonly used public data, we identified TCR-epitope specificities using Repertoire Immune Medicine’s DECODE™ platform yielding interactions between over 10M TCRs and thousands of epitopes as measured from patient samples across disease states in a manner consistent with [9]. Here, full TCR sequences were generated directly. To enable a contrastive framework, we selected only positive TCR-epitope pairs from these data with the highest confidence epitope recognition, representing approximately 0.0005% of all measured interactions. This ultimately yielded a dataset with approximately 7 \times the epitope diversity of other sources.

We split the resulting dataset (“R-1”) by first holding all TCRs in the TULIP test dataset out for testing. We assigned TCRs pairing with epitopes that had two or fewer TCRs to the training dataset, for maximal training diversity. We split all remaining unique TCRs for each epitope into training (70%), validation (15%) and held-out test (15%). Following data splitting, we confirmed that no TCRs occurred in multiple dataset splits, and that each TCR-epitope pair was unique. R-1 dataset composition was found to be diverse and less dependent on any individual epitope (Tab. 1). As is common in contrastive learning, we treated all non-positive TCR-epitope interactions as implicitly negative pairs. We did not provide MHC information to our model or use the MHC in constructing the loss, treating the peptide as the sole representative of the pMHC epitope. Less than 6.5% of peptides were presented by more than one MHC molecule; we therefore speculated that adding MHC identity would not be required for pMHC recognition (as in [10]).

2.2 Model Architecture

We constructed a simple contrastive learning model for mapping TCR-epitope reactivity (shown in Fig. 1A). Briefly, an epitope is encoded by passing the peptide sequence through an ESM-2 encoder followed by an attention pooling and a linear projection into the latent space [14]. A TCR is encoded by passing the amino acid sequence for the alpha and beta subunits through respective ESM-2 encoders, followed by attention pooling, concatenation, and projection into the latent space. The third complementarity-determining region (CDR3) of each TCR subunit is thought to be the primary (but not sole) driver of TCR-epitope binding [3], thus, we trained models that encoded the CDR3 alone as well as the full TCR sequence. Training and implementation details are provided in Section A.2.

Table 2: evaluation metrics for REPTRA, TULIP [15], and ImmuneCLIP [10] on the TULIP and R-1 test datasets. All values are macro AUROCs. We report performance on the TULIP test dataset as a benchmark, however 568/853 (66%) of TULIP test TCRs were also in the ImmuneCLIP train split (see Section A.4). Thus, there is significant leakage inflating ImmuneCLIP performance. Note that REPTRA cannot be applied to the TULIP test dataset, which lacks non-CDR3 information.

Model	TULIP Test		R-1 Test	
	T-AUROC	I-AUROC	D-AUROC	
REPTRA	-	0.967	0.886	
REPTRA-CDR3	0.805	0.942	0.820	
TULIP	0.732	0.887	0.762	
ImmuneCLIP	0.804*	0.751	0.676	

2.3 Code Availability

TCR-epitope affinity data will not be shared due to patient privacy and IP considerations. Code for training and evaluating REPTRA are available on GitHub under a noncommercial license at: <https://github.com/reptoireimmunemedicines/reptra>.

3 Experiments and Results

3.1 Scaling TCR-Epitope Contrastive Learning

We tested whether TCR-epitope contrastive learning was limited by data or by encoder model capacity by training REPTRA architectures using ESM-2 backbones from 8M to 150M parameters (Tab. A2). We compared validation loss and debiased AUROC between these backbones to identify potential scaling laws for TCR-epitope contrastive learning. Surprisingly, we found that increased backbone size and model capacity did not improve validation performance when training on CDR3 regions alone or on full TCR sequences (Fig. A1), indicating that even with a much larger dataset than previous studies and richer description of the TCR, we are limited by the diversity of the data. Furthermore, we observed the encoding full TCR sequences dramatically improved validation loss and AUROC. We selected the full-TCR REPTRA model with ESM-2 150M (“REPTRA”) and the CDR3 REPTRA model with ESM-2 150M (“REPTRA-CDR3”) for further evaluation due to slightly smoother training and for consistency between CDR3 and full-TCR models.

3.2 Model Evaluation and Benchmarking

We evaluated REPTRA alongside to two top-performing models in the literature on the publicly available TULIP test dataset and our R-1 test dataset (Tab. 2). Benchmarking is a known challenge for ML models of TCR-epitope recognition, as each model has been trained on TCRs paired with different epitopes, and there is known train-test leakage. We additionally used our full R-1 test dataset as a challenge to probe performance across a wider portion of epitope-space. We calculated AUROC for TULIP test using the exact TULIP negatives (T-AUROC), and for R-1 test using both the confusion matrix as in the InfoNCE loss (I-AUROC) and deduplicated as in the debiased InfoNCE loss (D-AUROC). As in the scaling experiments, REPTRA outperforms REPTRA-CDR3 indicating that non-CDR3 regions contribute to binding prediction. REPTRA and REPTRA-CDR3 outperform comparator models in the literature, even outperforming TULIP on the TULIP test dataset. The less-performant REPTRA-CDR3 (with full representation ablated) still performs comparably to ImmuneCLIP on the TULIP test dataset, even though 568/853 (66%) of TULIP test TCRs appear in the ImmuneCLIP training dataset due to leakage in data splitting (see Section A.4 for a longer discussion). Thus, our approach with REPTRA is superior to previous models.

3.3 Ablation Experiment

We performed an ablation study to better understand the contributions of debiased InfoNCE loss and full-TCR representation, reporting validation D/I-Loss and D/I-AUROC, and test D/I-AUROC. We ablated the debiased InfoNCE loss (A1, replacing it with standard InfoNCE and using InfoNCE loss

Table 3: ablations of REPTRA. We replaced debiased InfoNCE with standard InfoNCE and the full-TCR sequence with only CDR3s.

Model (Ablation)	R-1 Validation				R-1 Test	
	I-Loss	I-AUROC	D-Loss	D-AUROC	I-AUROC	D-AUROC
REPTRA (None)	3.65	0.963	5.59	0.867	0.967	0.886
A1 (InfoNCE)	3.54	0.933	5.84	0.844	0.946	0.864
A2 (InfoNCE/CDR3)	3.89	0.857	6.31	0.762	0.896	0.787

as the model selection criterion), and both debiased InfoNCE and the full-TCR representation (A2, replacing it with the typical CDR3-alone encoding). Results in Tab. 3 indicate that each of these adjustments to the model contribute to its overall performance. Interestingly, using the debiased loss improves model performance on the standard InfoNCE-style AUROC, supporting the notion that including duplicated comparisons distorts the learned latent space.

3.4 Interpreting REPTRA Attention

We initialized the attention pooling weights within REPTRA to be a mean pool. During training, the model learns to attend to the regions of the sequence useful for determining epitope specificity. Because non-CDR3 information from the full TCR sequence was found to contribute to model performance, it is of interest to determine how REPTRA attends to the full TCR sequences. We tested this by extracting the weights from attention pooling on TCRs within the test dataset (Fig. A2). We found that in addition to CDR3s, TCR sequence regions consistent with CDR1/CDR2 positions are weighted higher during attention pooling than the framework regions throughout, especially for the TCR beta chain. We investigated further by structurally modeling a GILGFVFTL-binding TCR and mapping the attention weights for that TCR onto its structure (shown in Fig. A2B) [6, 19]. We found that the highest-attention regions were those oriented toward the pMHC complex. When reviewing the GILGFVFTL-binding TCR, we found an additional high-attention region corresponding to the sequence REKKESFPL within the Framework-3 region of the beta chain (IMGT positions 80-87), which has previously been referred to as “CDR2.5,” and may contact the epitope [5].

3.5 Limitations

A limitation in this study (and to-date all other studies of TCR-epitope recognition) is sparse coverage of the epitope space, as indicated by lack of performance improvement with larger encoder backbones. Although our R-1 dataset includes approximately $7\times$ the diversity of literature examples, this represent a small fraction of known epitope space. Furthermore, our model does not incorporate MHC information, though we plan to jointly encode this with the peptide in the future. Because most peptides are only presented by one MHC, we did not add this representation to our initial model.

4 Conclusion

We have presented two modifications to the TCR-pMHC contrastive learning problem: representation of the full TCR sequence and a modified contrastive loss function. Our approach yields improved model performance and enables interpretation of model weights in a way that is consistent with known biology. Furthermore, it indicates that existing datasets lacking information outside the CDR3 may not be optimal for developing TCR-epitope ML models. It would be of interest to apply interpretability approaches to answer specific scientific questions, e.g. which epitope residues are recognized by a TCR (to thus identify undesirable cross-reactivity), or determine whether one or more CDR motifs is associated with recognizing a given epitope. Future work in this space may benefit most significantly from a more diverse set of TCR-pMHC training data, broadly covering self-antigens presented in Class I and Class II MHCs in addition to the limited set of well-understood viral epitopes, with the ultimate goal of enabling broad generalization beyond known epitopes. To this end, we plan to scale by leveraging a larger fraction of our TCR-pMHC interaction database toward developing a broadly generalizable model.

Acknowledgments and Disclosure of Funding

We gratefully thank the Lab Platform team at Repertoire Immune Medicines (Amy Perea, Genesis Tejada, Del Leistritz-Edwards, William Ruff, Qiaomu Tian, Jack Prazich, Veronica Sanchez, Katherine Triebel, Marcos Wille, Manning DelCogliano, and Preet Joshi) for data acquisition and biological direction. We additionally thank the Computational Engineering team (Kane Hadley, Elysha Sameth, Aswathy Sheena, and George Regas) for ML Ops and data support.

JA, BV, NP, AC, CB, and DC are employed by and/or have received equity in Repertoire Immune Medicines, Inc.

References

- [1] Meriem Attaf, Eric Huseby, and Andrew K Sewell. $\alpha\beta$ t cell receptors as predictors of health and disease. *Cellular & molecular immunology*, 12(4):391–399, 2015.
- [2] Xavier Brochet, Marie-Paule Lefranc, and Véronique Giudicelli. Imgt/v-quest: the highly customized and integrated system for ig and tr standardized vj and vdj sequence analysis. *Nucleic acids research*, 36(suppl_2):W503–W508, 2008.
- [3] Lukasz K Chlewicki, Phillip D Holler, Bridget C Monti, Matthew R Clutter, and David M Kranz. High-affinity, peptide-specific t cell receptors can be generated by mutations in cdr1, cdr2 or cdr3. *Journal of molecular biology*, 346(1):223–239, 2005.
- [4] Giancarlo Croce, Sara Bobisse, Dana Léa Moreno, Julien Schmidt, Philippe Guillame, Alexandre Harari, and David Gfeller. Deep learning predictions of tcr-epitope interactions reveal epitope-specific chains in dual alpha t cells. *Nature Communications*, 15(1):3211, 2024.
- [5] Pradyot Dash, Andrew J Fiore-Gartland, Tomer Hertz, George C Wang, Shalini Sharma, Aisha Souquette, Jeremy Chase Crawford, E Bridie Clemens, Thi HO Nguyen, Katherine Kedzierska, et al. Quantifiable predictive features define epitope-specific t cell receptor repertoires. *Nature*, 547(7661):89–93, 2017.
- [6] Warren L DeLano et al. Pymol: An open-source molecular graphics tool. *CCP4 Newslett. protein crystallogr.*, 40(1):82–92, 2002.
- [7] Omar NA Demerdash, Jeremy C Smith, et al. Tcr-h: explainable machine learning prediction of t-cell receptor epitope binding on unseen datasets. *Frontiers in Immunology*, 15:1426173, 2024.
- [8] Ceder Dens, Wout Bittremieux, Fabio Affaticati, Kris Laukens, and Pieter Meysman. Interpretable deep learning to uncover the molecular binding patterns determining tcr-epitope interaction predictions. *ImmunoInformatics*, 11:100027, 2023.
- [9] Joshua M Francis, Del Leistritz-Edwards, Augustine Dunn, Christina Tarr, Jesse Lehman, Conor Dempsey, Andrew Hamel, Violeta Rayon, Gang Liu, Yuntong Wang, et al. Allelic variation in class i hla determines cd8+ t cell repertoire shape and cross-reactive memory responses to sars-cov-2. *Science immunology*, 7(67):eabk3070, 2021.
- [10] Chiho Im, Ryan Zhao, Scott D Boyd, and Anshul Kundaje. Sequence-based tcr-peptide representations using cross-epitope contrastive fine-tuning of protein language models. In *International Conference on Research in Computational Molecular Biology*, pages 34–48. Springer, 2025.
- [11] Yuepeng Jiang, Miaoze Huo, and Shuai Cheng Li. Teinet: a deep learning framework for prediction of tcr-epitope binding specificity. *Briefings in bioinformatics*, 24(2):bbad086, 2023.
- [12] Diederik P Kingma and Jimmy Ba. Adam: A method for stochastic optimization. *arXiv preprint arXiv:1412.6980*, 2014.
- [13] Christian Klein, Ulrich Brinkmann, Janice M Reichert, and Roland E Kontermann. The present and future of bispecific antibodies for cancer therapy. *Nature reviews Drug discovery*, 23(4):301–319, 2024.
- [14] Zeming Lin, Halil Akin, Roshan Rao, Brian Hie, Zhongkai Zhu, Wenting Lu, Nikita Smetanin, Robert Verkuil, Ori Kabeli, Yaniv Shmueli, et al. Evolutionary-scale prediction of atomic-level protein structure with a language model. *Science*, 379(6637):1123–1130, 2023.
- [15] Barthelemy Meynard-Piganeau, Christoph Feinauer, Martin Weigt, Aleksandra M Walczak, and Thierry Mora. Tulip: A transformer-based unsupervised language model for interacting peptides and t cell receptors that generalizes to unseen epitopes. *Proceedings of the National Academy of Sciences*, 121(24):e2316401121, 2024.

- [16] Mark R Middleton, Cheryl McAlpine, Victoria K Woodcock, Pippa Corrie, Jeffrey R Infante, Neil M Steven, Thomas R Jeffry Evans, Alan Anthoney, Alexander N Shoushtari, Omid Hamid, et al. Tebentafusp, a tcr/anti-cd3 bispecific fusion protein targeting gp100, potently activated antitumor immune responses in patients with metastatic melanoma. *Clinical Cancer Research*, 26(22):5869–5878, 2020.
- [17] Yuta Nagano, Andrew GT Pyo, Martina Milighetti, James Henderson, John Shawe-Taylor, Benny Chain, and Andreas Tiffreau-Mayer. Contrastive learning of t cell receptor representations. *Cell Systems*, 16(1), 2025.
- [18] Aaron van den Oord, Yazhe Li, and Oriol Vinyals. Representation learning with contrastive predictive coding. *arXiv preprint arXiv:1807.03748*, 2018.
- [19] Saro Passaro, Gabriele Corso, Jeremy Wohlwend, Mateo Reveiz, Stephan Thaler, Vignesh Ram Somnath, Noah Getz, Tally Portnoi, Julien Roy, Hannes Stark, et al. Boltz-2: Towards accurate and efficient binding affinity prediction. *BioRxiv*, pages 2025–06, 2025.
- [20] Adam Paszke, Sam Gross, Francisco Massa, Adam Lerer, James Bradbury, Gregory Chanan, Trevor Killeen, Zeming Lin, Natalia Gimelshein, Luca Antiga, et al. Pytorch: An imperative style, high-performance deep learning library. *Advances in neural information processing systems*, 32, 2019.
- [21] Mikhail Shugay, Dmitriy V Bagaev, Ivan V Zvyagin, Renske M Vroomans, Jeremy Chase Crawford, Garry Dolton, Ekaterina A Komech, Anastasiya L Sycheva, Anna E Koneva, Evgeniy S Egorov, et al. Vdjdb: a curated database of t-cell receptor sequences with known antigen specificity. *Nucleic acids research*, 46(D1):D419–D427, 2018.
- [22] Sylvain Simon, Grace Bugos, Rachel Prins, Anusha Rajan, Arulmozhi Palani, Kersten Heyer, Andrew Stevens, Longhui Zeng, Kirsten A Thompson, Pinar A Atilla, et al. Design of sensitive monospecific and bispecific synthetic chimeric t cell receptors for cancer therapy. *Nature Cancer*, pages 1–19, 2025.
- [23] Nili Tickotsky, Tal Sagiv, Jaime Prilusky, Eric Shifrut, and Nir Friedman. Mcpas-tcr: a manually curated catalogue of pathology-associated t cell receptor sequences. *Bioinformatics*, 33(18):2924–2929, 2017.
- [24] Randi Vita, Nina Blazeska, Daniel Marrama, IEDB Curation Team Members Shackelford Deborah Zalman Leora Foos Gabriele Zarebski Laura Chan Kenneth Reardon Brian Fitzpatrick Sidne Busse Matthew Coleman Sara Sedwick Caitlin Edwards Lindy MacFarlane Catriona Ennis Marcus, Sebastian Duesing, Jason Bennett, Jason Greenbaum, Marcus De Almeida Mendes, Jarjapu Mahita, Daniel K Wheeler, et al. The immune epitope database (iedb): 2024 update. *Nucleic Acids Research*, 53(D1):D436–D443, 2025.

A Technical Appendices and Supplementary Material

A.1 Supplementary Figures

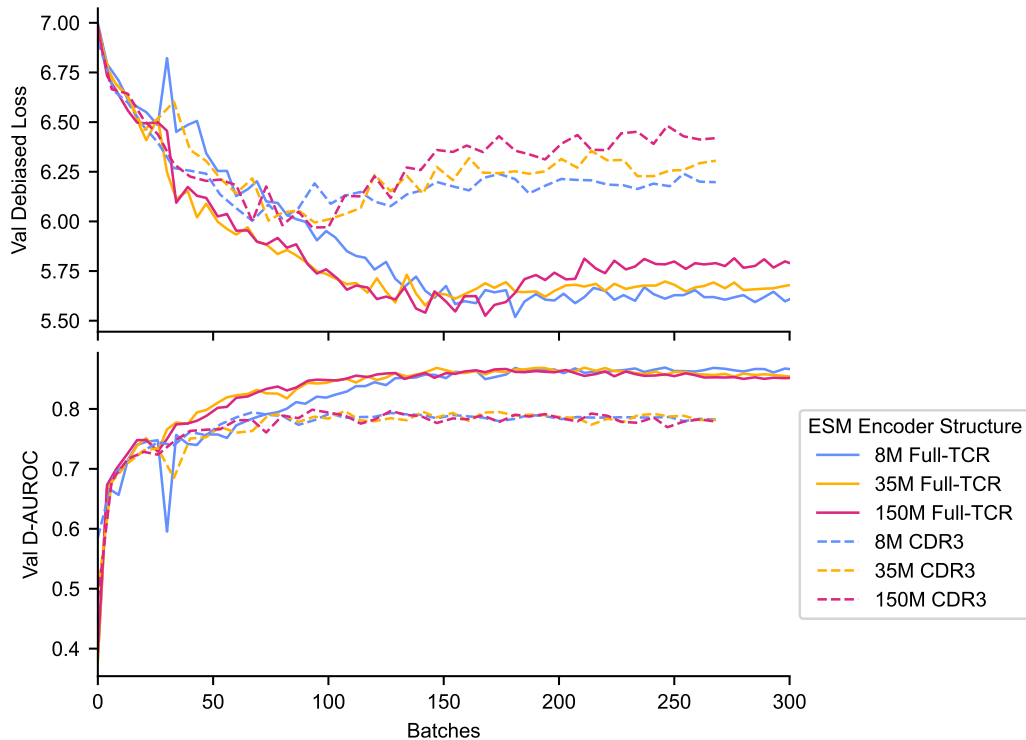
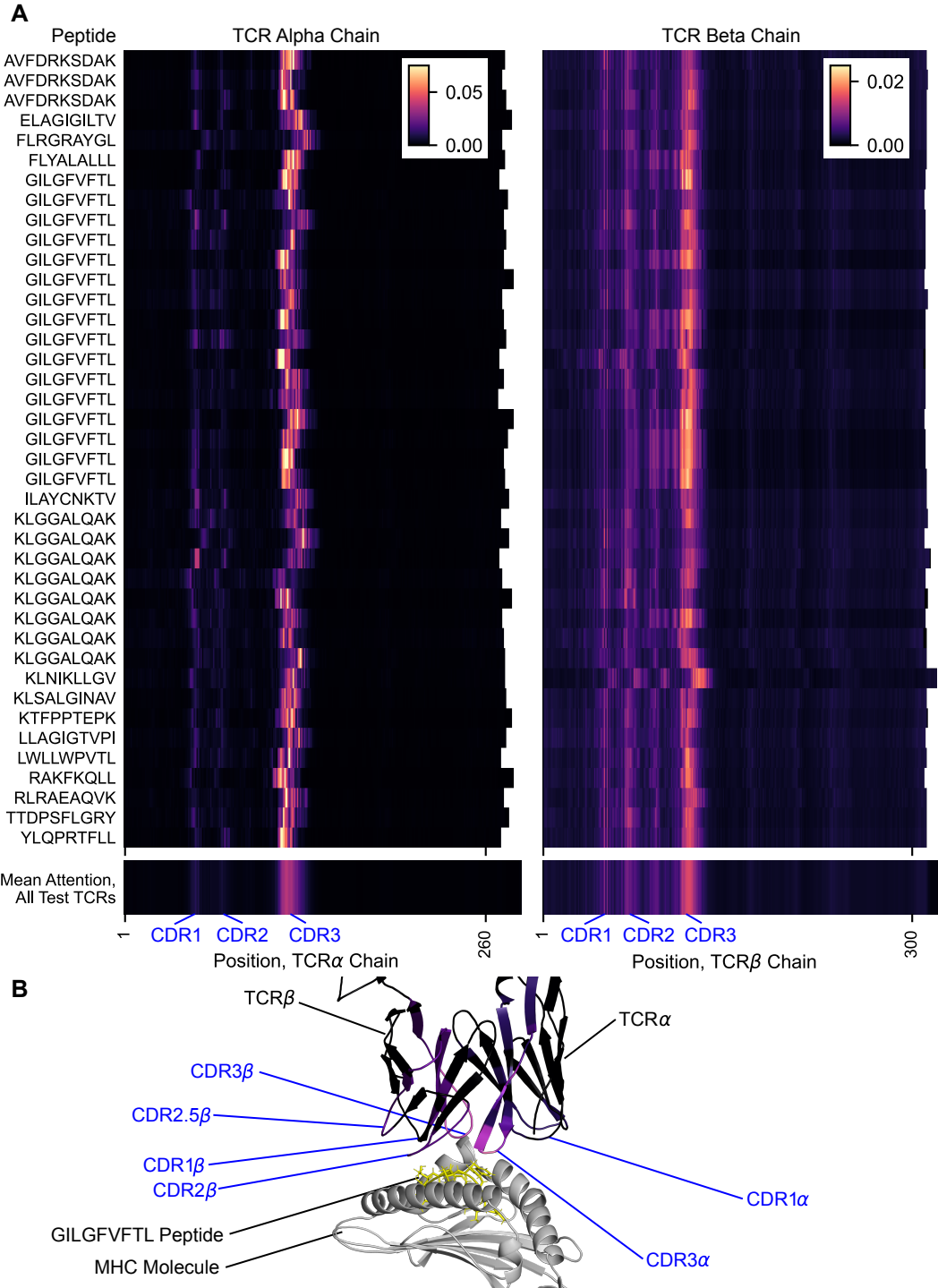


Figure A1: scaling REPTRA encoders. We show performance vs. batch (optimizer step) because tokens per batch varies approximately 10-fold depending on whether the full TCR or CDR3-only is used.



A.2 Training and Implementation Details

All models were developed in PyTorch [20] and trained in a consistent manner using the AdamW optimizer [12] with hyperparameters provided in Tab. A1. An epitope-frequency-debiased InfoNCE loss was defined and used for model fitting, as detailed in Section A.3. We selected the best model for each training run using the debiased InfoNCE AUROC on the validation split. We defined the total number of tokens used per training run as the sum of the epitope and TCR tokens for each TCR-epitope pair passed through the model. All models were trained on a single NVIDIA A10 GPU using mixed precision; a training run was complete in approximately 5 hr for a full-TCR model or 1 hr for a CDR3-only model.

A.3 Debiased InfoNCE Loss

A standard approach in contrastive learning is to use the InfoNCE loss [18]. Here, for each batch of N positive pairs, a similarity matrix is constructed of dimension $N \times N$ (where each anchor forms a row and each candidate forms a column). Cross-entropy is applied with the diagonal element typically considered the correct class. In bimodal settings, this is done in both directions and the losses are averaged. Equivalently, during evaluation, the $N \times N$ matrix is constructed and used to compute performance metrics (e.g. AUROC). It is established that many unique TCRs bind to the same epitope. Previous studies have addressed this by incorporating off-diagonal positives in the confusion matrix, up/downsampling, and maintaining a low batch size during training [10]. However, contrastive learning generally benefits from large batch sizes to learn the representation space, so keeping additional TCR diversity is helpful even for common epitopes. We further speculated that training using an InfoNCE-style similarity matrix would lead to distortion of the representation space due to duplicated comparisons with the same epitope.

If an epitope e_a forms positive pairs with k TCRs, in the InfoNCE confusion matrix, the number of positive and negative entries for e_a are given by:

$$N_{e_a}^+ = k^2, \text{ and} \quad (1)$$

$$N_{e_a}^- = k(N - k) \quad (2)$$

where the k unique positive TCRs and $N - k$ unique negative TCRs are compared to epitope e_a a total of k times. During training common epitopes will dominate the representation due to nonlinear scaling with k (visualized in Fig. 1B) and during evaluation, the same negatives and positives may be over-counted in computing evaluation loss or other metrics. This results in apparently strong model performance even for TCRs that bind rare epitopes, but may be attributable to multiple comparisons with the same common negative epitope.

We developed a debiased InfoNCE loss by simply deduplicating epitopes and TCRs when constructing the InfoNCE-style confusion matrix. Using this approach, the number of positive and negative entries for e_a are given by:

$$N_{e_a}^+ = k, \text{ and} \quad (3)$$

$$N_{e_a}^- = N - k \quad (4)$$

respectively. This enables larger batch sizes during training and ensures non-duplication of exact TCR-epitope comparisons during evaluation.

A.4 Data Splitting and Leakage

Prior studies have struggled to maintain consistent data splits in this space, in addition to the challenge of proper negative sampling. Here, we chose to treat the TULIP test dataset [15] as a true benchmark, rather than attempt to re-split such that all epitopes were seen by each model (as in [10] and elsewhere), in order to stay true to the spirit of a benchmark, i.e. so that all models can be evaluated on the exact same data.

This approach leads to one additional challenge: potential data leakage for models that are not explicitly split consistently with TULIP in mind (i.e. ImmuneCLIP). ImmuneCLIP previously addressed this challenge by removing “all epitope/TCR pairs in each of the test sets that [the] model had seen during training.” Implicitly, *ImmuneCLIP retained TCRs that were seen during training but were paired with different epitopes; thus it has been trained on some of the TCRs in*

negative TCR-epitope pairs in TULIP. We found that 568 of 853 TULIP test TCRs were in the ImmuneCLIP train split. Even if paired with different negative epitopes in the TULIP test dataset, the ImmuneCLIP model has seen that these TCRs are positive for other epitopes during training; thus there is significant information leakage that lends a positive bias to ImmuneCLIP. We nevertheless report the ImmuneCLIP performance here, as a conservative upper bound on the method, and show that our approach nevertheless shows improvement vs literature state-of-the-art.

A.5 Training Hyperparameters

For all model training, hyperparameters were held fixed with the exception of the maximal number of training tokens per run (and the evaluation interval), as noted, due to the tokens-per-sequence varying approximately tenfold between CDR3-only and full-TCR representations.

Table A1: training hyperparameter values for training REPTRA.

Hyperparameter	Value
Minibatch Size	128
Accumulation Steps	8
Learning Rate	10^{-3}
Training Tokens (Full TCR)	2.5×10^{10}
Training Tokens (CDR3)	2.5×10^9
Warmup Fraction	0.05
Decay Fraction	1.0
Minimum Learning Rate	0
Weight Decay	10^{-3}
Temperature	0.07
Stopping Metric	D-AUROC
Patience (Epochs)	10

A.6 Model Architectures

Table A2: model architectures tested for scaling REPTRA. Only the final transformer is fine-tuned.

Model	ESM-2 Backbone	Projection Head	Embedding Dimension	Trainable Parameters	Total Parameters
REPTRA	8M	Attention Pooling	256	3.9M	22.8M
	35M	Attention Pooling	256	8.7M	100.9M
	150M	Attention Pooling	256	15.3M	444.9M